Supplementary materials of the article "Generalized Graetz problem in circular tube with a mass transfer coupling between the solid and the liquid"

F. Pigeonneau[a,*], B. Jaffrennou[b], A. Letailleur[b], K. Limouzin[c]

[a]*Surface du Verre et Interfaces, UMR 125 CNRS/Saint-Gobain, 39 quai Lucien Lefranc – BP 135, 93303 Aubervilliers cedex, France*
[b]*Saint-Gobain Recherche, 39 quai Lucien Lefranc – BP 135, 93303 Aubervilliers cedex, France*
[c]*Saint-Gobain Performance Plastics, Z.I. de Chesnes, 5 rue du Dauphiné, 38297 Saint-Quentin Fallavier, France*

Abstract

This supplementary material describes the numerical methods implemented to solve problems described in the article titled "Numerical investigation of a generalized Graetz problem in circular tube with a mass transfer coupling between the solid and the liquid". In section 1, a dedicated numerical tool to solve the conjugated problem with a difference finite/pseudo spectral method has been developed. The numerical accuracy is also provided. The numerical method for the conjugated static migration is given in section 2.

Keywords: Graetz problem, migration, plasticizer, food safety, contamination

1. Numerical method of the conjugated dynamic migration problem

Notation used in this supplementary material is not recalled here. The reader is referred to the article associated to this document.

Recall that in dynamic condition, the conjugated problem of migration is constituted by the ordinary differential equation

$$\frac{d\langle C_f\rangle(z;t)}{dz} = \frac{2\,\mathrm{Sh}(\mathrm{Gr},z)}{\mathrm{Gr}}\left[C_f(1,z;t) - \langle C_f\rangle(z;t)\right], \tag{1}$$

*Corresponding author: Tel. +33 (1) 48 39 59 99, Fax +33 (1) 48 39 55 62.
Email addresses: franck.pigeonneau@saint-gobain.com (F. Pigeonneau), boris.jaffrennou@saint-gobain.com (B. Jaffrennou), alban.letailleur@saint-gobain.com (A. Letailleur), krystel.limouzin@saint-gobain.com (K. Limouzin)

with the boundary condition

$$\langle C_f \rangle(0;t) = 0. \tag{2}$$

Mass concentration $C_p(\zeta, t; z)$ in the solid tube verifies the unsteady diffusion equation

$$\frac{\partial C_p}{\partial t} = \frac{1}{1+\Delta r\zeta}\frac{\partial}{\partial \zeta}\left[(1+\Delta r\zeta)\frac{\partial C_p}{\partial \zeta}\right], \tag{3}$$

with the following boundary conditions

$$\frac{\partial C_p}{\partial \zeta}(0,t;z) = \alpha\,\mathrm{Sh}(\mathrm{Gr},z)\left[C_p(0,t;z) - \langle C_f\rangle(z;t)\right], \tag{4}$$

$$\frac{\partial C_p}{\partial \zeta}(1,t;z) = 0, \tag{5}$$

and initial condition

$$C_p(\zeta, 0; z) = 1. \tag{6}$$

1.1. Numerical discretizations in space and time

To determine the plasticizer concentration in the tube and the average concentration migrating in the liquid, the ordinary differential equation given by (1) and the partial differential equation (3) have to be solved together numerically. For both concentrations, $\langle C_f\rangle(z;t)$ and $C_p(\zeta,t;z)$, the discretization over the axial position is achieved by using a uniform grid where nodal points are given by

$$z_i = \frac{i}{N_z}, \text{ for } i = 0 \text{ to } N_z. \tag{7}$$

The size of the grid is consequently equal to $\delta z = 1/N_z$. Also, the time is discretized using a constant time step, δt meaning that the time at n-th iteration is given by

$$t_n = n\delta t. \tag{8}$$

First the discretization of the ordinary differential equation of $\langle C_f\rangle(z;t)$ is considered. Let $\langle C_f\rangle_i^n$ the average concentration of plasticizer in the liquid at the time step n for the longitudinal position z_i:

$$\langle C_f\rangle_i^n = \langle C_f\rangle(z_i; t_n), \tag{9}$$

and $C_{p,i}^n(\zeta)$ the concentration of plasticizer in the PVC tube at the time step n and at the discrete position z_i:

$$C_{p,i}^n(\zeta) = C_p(\zeta, t_n; z_i), \tag{10}$$

which is at this stage yet a continuous function of ζ.

To determine the first derivative respect to z of $\langle C_f \rangle(z;t)$, a backward differentiation formula at the second order (BDF-2) in δz is used [1, 2]:

$$\frac{d\langle C_f \rangle(z_i;t_n)}{dz} = \frac{3\langle C_f \rangle_i^n - 4\langle C_f \rangle_{i-1}^n + \langle C_f \rangle_{i-2}^n}{2\delta z} + \mathcal{O}(\delta z^2), \tag{11}$$

when i is greater or equal to 2 otherwise an Euler scheme accurate at the first order is used when $i = 1$:

$$\frac{d\langle C_f \rangle(z_1;t_n)}{dz} = \frac{\langle C_f \rangle_1^n - \langle C_f \rangle_0^n}{\delta z} + \mathcal{O}(\delta z). \tag{12}$$

From these two relations, the average concentration of plasticizer in the liquid for each grid point z_i is given by

$$\langle C_f \rangle_1^n = \frac{2\,\mathrm{Gr}^{-1}\,\mathrm{Sh}(\mathrm{Gr}, z_1)\delta z C_{p,1}^n(0) - \langle C_f \rangle_0^n}{1 + 2\,\mathrm{Gr}^{-1}\,\mathrm{Sh}(\mathrm{Gr}, z_1)\delta z} \tag{13a}$$

in $i = 1$ and

$$\langle C_f \rangle_i^n = \frac{4\,\mathrm{Gr}^{-1}\,\mathrm{Sh}(\mathrm{Gr}, z_i)\delta z C_{p,i}^n(0) + 4\langle C_f \rangle_{i-1}^n - \langle C_f \rangle_{i-2}^n}{3 + 4\,\mathrm{Gr}^{-1}\,\mathrm{Sh}(\mathrm{Gr}, z_1)\delta z} \tag{13b}$$

for $2 \leq i \leq N_z$.

Now turn on the discretization of the diffusion equation of $C_{p,i}^n(\zeta)$. First, the time derivative of equation (3) is determined with the backward differentiation formula at the second order in time, BDF-2 [1, 2]. In this way, the plasticizer concentration in the solid, $C_{p,i}^n(\zeta)$, obeys an Helmholtz equation written as follows

$$\frac{3}{2\delta t} C_{p,i}^{n+1} - \frac{\Delta r}{1 + \Delta r \zeta} \frac{\partial C_{p,i}^{n+1}}{\partial \zeta} - \frac{\partial^2 C_{p,i}^{n+1}}{\partial \zeta^2} = \frac{4C_{p,i}^n - C_{p,i}^{n-1}}{2\delta t}, \tag{14}$$

for all i, $n > 0$ and for $\zeta \in]0;1[$. The initial conditions are simply given by

$$C_{p,i}^{0}(\zeta) = 1, \ \forall \ i. \tag{15}$$

For the boundary conditions, the relations (13a) and (13b) are used to transform equation (4) written in $\zeta = 0$ in Robin condition as follows

$$\frac{\partial C_{p,1}^{n+1}}{\partial \zeta} - \frac{\alpha \, \mathrm{Sh}(\mathrm{Gr}, z_1)}{1 + 2 \, \mathrm{Gr}^{-1} \, \mathrm{Sh}(\mathrm{Gr}, z_1) \delta z} C_{p,1}^{n+1} = - \frac{\alpha \, \mathrm{Sh}(\mathrm{Gr}, z_1) \langle C_f \rangle_1^{n+1}}{1 + 2 \, \mathrm{Gr}^{-1} \, \mathrm{Sh}(\mathrm{Gr}, z_1) \delta z}, \tag{16a}$$

in $i = 1$ and

$$\frac{\partial C_{p,i}^{n+1}}{\partial \zeta} - \frac{3\alpha \, \mathrm{Sh}(\mathrm{Gr}, z_i)}{3 + 4 \, \mathrm{Gr}^{-1} \, \mathrm{Sh}(\mathrm{Gr}, z_1) \delta z} C_{p,i}^{n+1} = - \frac{\alpha \, \mathrm{Sh}(\mathrm{Gr}, z_1) (4 \langle C_f \rangle_{i-1}^{n+1} - \langle C_f \rangle_{i-2}^{n+1}}{3 + 4 \, \mathrm{Gr}^{-1} \, \mathrm{Sh}(\mathrm{Gr}, z_1) \delta z}, \tag{16b}$$

for $2 \leq i \leq N_z$.

To solve the Helmholtz problem, a pseudo-spectral method is used based on Chebyshev polynomial. A collocation method is used to evaluate the continuous Helmholtz equation for which $N_\zeta + 1$ collocation points are distributed following the Gauss-Lobatto points as follows

$$\zeta_j = \frac{1}{2} \left[1 - \cos(j\pi / N_\zeta) \right], \ \text{for } j = 0 \text{ to } N_\zeta. \tag{17}$$

In the following $C_{p,i,j}^{n}$ is the value of the plasticizer concentration in the solid tube in z_i and ζ_j at the step time n. The first and second derivatives in each collocation point are given by [3]

$$\frac{\partial C_{p,i}^{n}}{\partial \zeta}(\zeta_j) = \sum_{k=0}^{N_\zeta} D_{jk} C_{p,i,k}^{n}, \tag{18}$$

$$\frac{\partial^2 C_{p,i}^{n}}{\partial \zeta^2}(\zeta_j) = \sum_{k=0}^{N_\zeta} D_{jk}^{2} C_{p,i,k}^{n}. \tag{19}$$

The matrix $\boldsymbol{D}$ is given in the book [3] for collocation points spreading over an interval between -1 to 1. In our case, the derivative matrix has to be multiplied by a factor 2 to take into account that $\zeta \in [0;1]$. The matrix $\boldsymbol{D}^2$ is obviously the square of the matrix $\boldsymbol{D}$.

From these developments, the determination of $C^n_{p,i,j}$ is achieved by solving the following linear problem:

For $j = 0$, i.e. $\zeta = 0$, the Robin condition becomes if $i = 1$:

$$\sum_{k=0}^{N_\zeta} \left[D_{jk} - \frac{\alpha\,\mathrm{Sh}(\mathrm{Gr}, z_1)}{1 + 2\,\mathrm{Gr}^{-1}\,\mathrm{Sh}(\mathrm{Gr}, z_1)\delta z}\delta_{jk} \right] C^{n+1}_{p,1,k} = -\frac{\alpha\,\mathrm{Sh}(\mathrm{Gr}, z_1)\langle C_f\rangle^{n+1}_1}{1 + 2\,\mathrm{Gr}^{-1}\,\mathrm{Sh}(\mathrm{Gr}, z_1)\delta z}, \tag{20a}$$

else if $2 \leq i \leq N_z$:

$$\sum_{k=0}^{N_\zeta} \left[D_{jk} - \frac{3\alpha\,\mathrm{Sh}(\mathrm{Gr}, z_i)}{3 + 4\,\mathrm{Gr}^{-1}\,\mathrm{Sh}(\mathrm{Gr}, z_1)\delta z}\delta_{jk} \right] C^{n+1}_{p,i,k} = -\frac{\alpha\,\mathrm{Sh}(\mathrm{Gr}, z_1)(4\langle C_f\rangle^{n+1}_{i-1} - \langle C_f\rangle^{n+1}_{i-2}}{3 + 4\,\mathrm{Gr}^{-1}\,\mathrm{Sh}(\mathrm{Gr}, z_1)\delta z}. \tag{20b}$$

In these two last relations, δ_{jk} is the Kronecker symbol.

For $1 \leq j \leq N_\zeta - 1$, the diffusion equation is written under a discrete form as follows

$$\sum_{k=0}^{N_\zeta} \left[\frac{3}{2\delta t}\delta_{jk} - \frac{\Delta r}{1 + \Delta r\zeta_j} D_{jk} - D^2_{jk} \right] C^{n+1}_{p,i,k} = \frac{4C^n_{p,i,j} - C^{n-1}_{p,i,j}}{2\delta t}. \tag{20c}$$

Finally, the cancellation of the flux in $\zeta = 1$, i.e. for $j = N_\zeta$, is given by

$$\sum_{k=0}^{N_\zeta} D_{jk} C^{n+1}_{p,i,k} = 0. \tag{20d}$$

This linear system is solved using a LU method for all grid points z_i spreading over the length of the tube. The solution of $C^{n+1}_{p,i,j}$ is further used to determine $\langle C_f\rangle^{n+1}_i$ using equations (13a) or (13b).

1.2. Numerical accuracy and truncation errors

In this subsection, the numerical consistency [4] and accuracy are tested by a comparison with an exact solution and a mesh convergence.

In order to compare to an exact solution, we point out that the plasticizer concentration in the solid tube at the entrance has a simple boundary conditions over the time leading to the knowledge of the concentration exactly. Indeed, at any time, the concentration C_p at the solid/liquid interface is always equal to zero and the flux is cancelled at the exterior of the tube. The exact solution of this problem in an hollow tube with initial

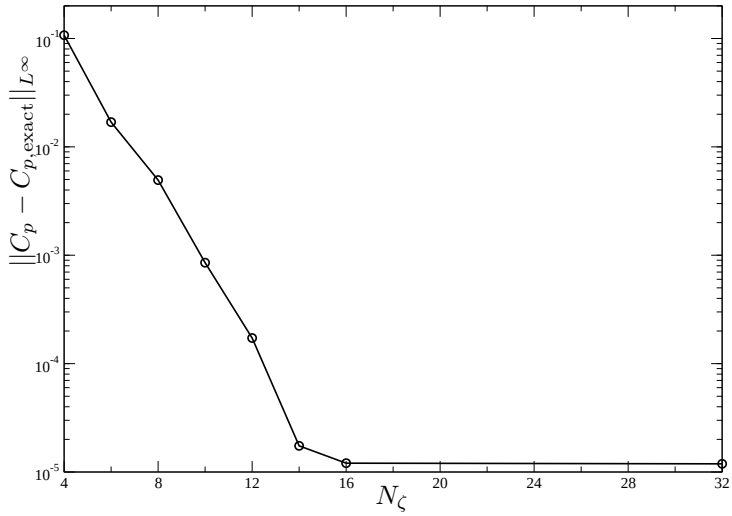

Figure 1: $||C_p - C_{p,\text{exact}}||_{L^\infty}$ as function of N_ζ in $z = 0$ for a particular case for which $K = 1$, $\Delta r = 10^{-1}$ and $\text{Gr} = 10^3$.

concentration equal to one has been determined by Carslaw and Jaeger [5] (see also [6]). It is given as a relation of Bessel functions as follows

$$C(r,t) = \pi \sum_{n=1}^{\infty} \frac{e^{-\Delta r^2 \alpha_n^2 t} J_1^2[\alpha_n(1+\Delta r)]\,[J_0(\alpha_n r)Y_0(\alpha_n) - Y_0(\alpha_n r)J_0(\alpha_n)]}{J_1^2[\alpha_n(1+\Delta r)] - J_0^2(\alpha_n)}, \tag{21}$$

with α_n solution of

$$J_0(\alpha_n)Y_1[\alpha_n(1+\Delta r)] - Y_0(\alpha_n)J_1[\alpha_n(1+\Delta r)] = 0. \tag{22}$$

In order to control the accuracy for increasing number of collocation points in the $\zeta-$space, we perform numerical simulations for a partition coefficient equal to unity and a Graetz number equal to 10^3. The time step has been taken equal to 10^{-5} and the axial coordinate of the tube is discretized with a mesh size equal to $4 \cdot 10^{-3}$. The error between the exact and numerical solutions has been determined in term of L^∞ norm and plotted in Figure 1 for increasing N_ζ. As expected for a spectral method, an exponential decrease of the error is observed when N_ζ rises up from 4 to 12. After, the error reaches an asymptotic value due to the error due to discretizations in time and in z coordinate.

To study the accuracy and the consistency in time discretization, numerical simulations

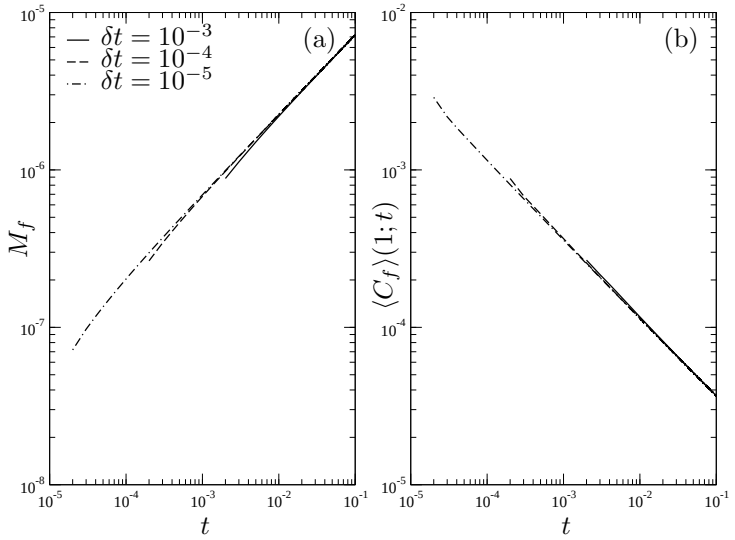

Figure 2: Time convergence test for a particular case for which $K = 1$, $\Delta r = 10^{-1}$ and $\mathrm{Gr} = 10^3$: (a) M_f vs. t and (b) $\langle C_f \rangle(1;t)$ vs. t.

have been done by decreasing time step over two orders of magnitude when the partition coefficient is unity and the Graetz number is equal to 10^3. Figure 2 presents on the left part the amount of plasticizer migrating in the liquid at the exit of the tube as a function of time. The right part of Figure 2 depicts the average plasticizer concentration at the exit of tube versus time. The number of collocation points has been taken equal to 64 and the mesh size in z coordinate is equal to $4 \cdot 10^{-4}$. Starting with a time step equal to 10^{-3}, numerical simulations have been done twice more by divided the time step by one order of magnitude. The example shows the numerical convergence. Remark a small difference only for the first time step.

In order to be more quantitative in the time convergence, it is possible to use an extrapolation method according to de Vahl Davis [7]. The order of truncation error can be estimated easily from the numerical solution. Assuming that a generic quantity, f, is given by

$$f_i = f_0 + C\delta t_i^{n_{\delta t}}, \tag{23}$$

in which f_i is the solution with a time step δt_i and f_0 is the solution when the time step goes to zero, $n_{\delta t}$ is the truncation error and C, a factor, assumed independent of the time step. It is possible by using three time steps such as $\delta t_1/\delta t_2 = \delta t_2/\delta t_3 = \lambda$ to evaluate

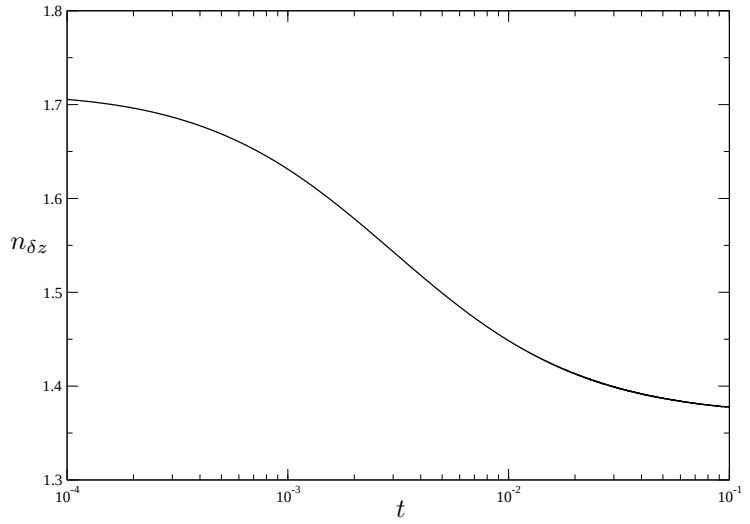

Figure 3: Exponent $n_{\delta z}$ of the truncation error as a function of t for $K = 1$, $\Delta r = 10^{-1}$ and $\mathrm{Gr} = 10^3$.

the truncation error by using the relation

$$n_{\delta t} = \ln\left(\frac{f_1 - f_2}{f_2 - f_3}\right) / \ln \lambda. \tag{24}$$

From the three numerical runs achieved for three decreasing time steps, we determine the value of M_f and $\langle C_f \rangle(1;t)$ when $t = 10^{-1}$. Using the previous relation, the truncation error in time is around 1 which is lesser than the order of scheme which is equal to 2. The result comes from that the first step can not evaluate as the second order which is sufficient to decrease the truncation error of one order.

Finally, the numerical truncation error has been estimated for the space discretization following z coordinate. For the same configuration, i.e. $K = 1$, $\Delta r = 10^{-1}$ and $\mathrm{Gr} = 10^3$, numerical simulations have been done for a time step equal to 10^{-5} and for 64 collocation points for the spectral method and for three decreasing mesh size, δz, equal to 1/50, 1/100 and 1/200. In this way, the truncation error in z-space, $n_{\delta z}$ can be estimated by an equivalent relation of (24). The exponent of the truncation error has been determined on the amount of plasticizer concentration, M_f, as a function of time. It is plotted in Figure 3 on which we remark that the truncation error decreases with time. At short times, the truncation error exponent is not to far from 2 in agreement with the order of discretization scheme. However, $n_{\delta z}$ decreases when the time increases to reach a value

close to 1.36 when $t = 10^{-1}$.

This closes the study of the numerical accuracy. The various numerical tests prove the consistency of the numerical method implemented to describe the coupled problem of migration in dynamic condition even if it is difficult to find the order of discretization schemes used in z-space and in time. In the application, the numerical simulations have been done with 64 collocation points for the discretization in ζ, $\delta t = 10^{-5}$ and $\delta z = 4 \cdot 10^{-3}$.

2. Numerical method of the static migration problem

Recall that the static migration problem is described by the diffusion equations in the solid and in the liquid as follows

$$\frac{\partial C_p}{\partial t} = \frac{1}{1+\Delta r\zeta}\frac{\partial}{\partial \zeta}\left[(1+\Delta r\zeta)\frac{\partial C_p}{\partial \zeta}\right], \tag{25}$$

$$\mathrm{Fo}\,\frac{\partial C_f}{\partial t} = \frac{1}{r}\frac{\partial}{\partial r}\left(r\frac{\partial C_f}{\partial r}\right). \tag{26}$$

The initial conditions are given by

$$C_p(\zeta, t) = 1, \text{ for } t = 0, \text{ and } \zeta \in]0;1[, \tag{27}$$

$$C_f(r, t) = 0, \text{ for } t = 0, \text{ and } r \in]0;1[, \tag{28}$$

and the boundary conditions by

$$\frac{\partial C_p(\zeta, t)}{\partial \zeta} = 0, \ \forall\, t > 0, \text{ and } \zeta = 1, \tag{29}$$

$$\left.\begin{array}{c} C_f = C_p, \\ \dfrac{\partial C_p}{\partial \zeta} = \alpha \dfrac{\partial C_f}{\partial r}. \end{array}\right\} \forall\, t > 0, \text{ and } \zeta = 0, r = 1. \tag{30}$$

Mathematically, this coupled equation system presented above can be solved exactly using for instance the Laplace transform [6]. The solution is usually expended as Bessel functions requiring the determination of the roots of relations of Bessel functions cumbersome to manipulate in practice. Consequently, a numerical method has been developed to solve the static migration problem. In order to do that, a pseudo-spectral method has

been developed taking into account the two mediums with interface conditions according to Guo et al. [3]. As already used to solve the conjugated dynamic problem, the time derivatives of $C_p(\zeta,t)$ and $C_f(r,t)$ are determined by the backward differentiation formula at the second order (so-called BDF-2 scheme) in time for which δt is the time step. The semi-discrete equations become

$$\frac{3C_p^{n+1}}{2\delta t} - \frac{\Delta r}{1+\Delta r\zeta}\frac{\partial C_p^{n+1}}{\partial \zeta} - \frac{\partial^2 C_p^{n+1}}{\partial \zeta^2} = \frac{4C_p^n - C_p^{n-1}}{2\delta t}, \tag{31}$$

$$\mathrm{Fo}\,\frac{3C_f^{n+1}}{2\delta t} - \frac{1}{r}\frac{\partial C_f^{n+1}}{\partial r} - \frac{\partial^2 C_f^{n+1}}{\partial r^2} = \mathrm{Fo}\,\frac{4C_f^n - C_f^{n-1}}{2\delta t}, \tag{32}$$

for which $C_p^{n+1}(\zeta) = C_p(\zeta, t_{n+1})$ and $C_f^{n+1}(r) = C_f(r, t_{n+1})$.

As previously done in section 1, a discretization of ζ-space is achieved following the Gauss-Lobatto distribution, see eq. (17). For the interior domain corresponding to the liquid, the second derivative respect to r is singular in $r = 0$. In order to avoid this singularity in discrete formulation and since only one boundary condition is required, the Gauss-Radau distribution is used such as r_p is given by [3]

$$r_p = \frac{1}{2}(1 + x_p), \text{ for } p = 0, \text{ to } N_r, \tag{33}$$

with

$$x_p = -\cos\left[\frac{(2p+1)\pi}{2N_r+1}\right], \text{ for } p = 0, \text{ to } N_r, \tag{34}$$

defined in the interval $]-1;1]$ leading that $r \in]0;1]$.

The determination of the first and second derivatives respect to x needs the knowledge of the differentiation matrix for the Gauss-Radau points, $\boldsymbol{D}_{GR}$. According to Guo et al. [3], this matrix is given as a function of the pseudo-spectral matrices as follows

$$\boldsymbol{D}_{GR} = \boldsymbol{T}_{GR} \cdot \hat{\boldsymbol{D}} \cdot \boldsymbol{T}_{GR}^{-1}, \tag{35}$$

for which $\boldsymbol{T}_{GR}$ and $\boldsymbol{T}_{GR}^{-1}$ are given page 17 and $\hat{\boldsymbol{D}}$ page 15 of [3].

The two semi-discrete balance equations, (31) and (32), are evaluated in each collocation points: in ζ_j for the solid domain and in r_p for the liquid domain apart from points

localized on the boundaries. From this method, the full discrete form is the following

$$\sum_{k=0}^{N_\zeta}\left[\frac{3}{2\delta t}\delta_{jk}-\frac{\Delta r}{1+\Delta r\zeta_j}D_{jk}-D_{jk}^2\right]C_{p,k}^{n+1}=\frac{4C_{p,j}^n-C_{p,j}^{n-1}}{2\delta t}\ \text{for } j=1 \text{ to } N_\zeta-1, \quad (36)$$

$$\sum_{l=0}^{N_r}\left[\mathrm{Fo}\,\frac{3}{2\delta t}\delta_{pl}-D_{r,pl}^{(2)}\right]C_{f,l}^{n+1}=\mathrm{Fo}\,\frac{4C_{f,p}^n-C_{f,p}^{n-1}}{2\delta t},\ \text{for } p=0 \text{ to } N_r-1, \quad (37)$$

$$\text{where } \boldsymbol{D}_r^{(2)}=4\left(\boldsymbol{D}_{GR}^2+\frac{1}{1+x}\boldsymbol{D}_{GR}\right). \quad (38)$$

To close the discrete system of equations, the boundary conditions are invoked. First, at the exterior boundary of the PVC tube, the cancellation of the mass flux is written as follows

$$\sum_{k=0}^{N_\zeta}D_{N_\zeta k}C_{p,k}^{n+1}=0. \quad (39)$$

The coupling the two domains is fully achieved by writing the boundary conditions in $\zeta=0$ and $r=1$ as follows

$$C_{p,0}-C_{f,N_r}=0, \quad (40)$$

$$\sum_{k=0}^{N_\zeta}D_{0k}C_{p,k}^{n+1}-\alpha\sum_{l=0}^{N_\zeta}D_{N_r l}C_{f,l}^{n+1}=0. \quad (41)$$

In this way, the fully coupled linear system is wholly built and solved by LU method. Once C_p and C_f have been computed at every time step, the average concentration of C_f given by

$$\langle C_f\rangle(t)=2\int_0^1 rC_f(r,t)dr, \quad (42)$$

is computed by an accurate quadrature using the Chebyshev decomposition as presented in chap. 2 of [3].

Since the numerical procedure is close to the method used for the dynamic condition, the numerical accuracy is not achieved a second time. In order to control the numerical accuracy, we compare with an exact solution when Δr is very small. Indeed, the problem written in cylindrical domain becomes close to the Cartesian situation since the curvature goes to zero. Furthermore, if the ratio of diffusion coefficients, D_f/D_p, is large the liquid domain could be considered as a perfect diffuser. This situation has been considered

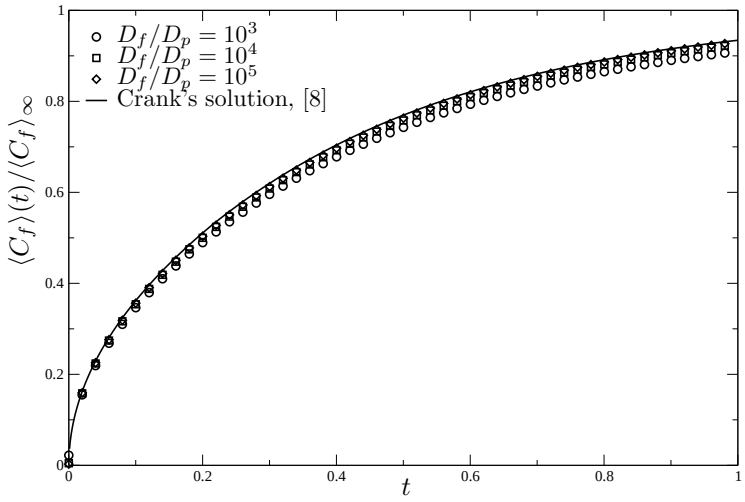

Figure 4: $\langle C_f\rangle(t)/\langle C_f\rangle_\infty$ as a function of time for $D_f/D_p = 10^3$, 10^4 and 10^5 when $\Delta r = 10^{-3}$ and $K = 1$. The solid line is the Crank's exact solution [8].

by Crank [8] for which only the diffusion process in the solid part is required. In this framework, Crank established an exact solution.

Numerical simulations have been done for a partition coefficient equal to one. The ratio Δr is set equal to 10^{-3}. Regarding the discretization in r and ζ, the numbers of collocation points have been taken equal to $N_r = 60$ and $N_\zeta = 100$ which can seem important. Nevertheless, since the value of α is very large, it is important to have a high resolution close to the PVC/liquid interface in order to satisfy the balance of fluxes, second relation of (30).

Figure 4 presents the profile of $\langle C_f\rangle(t)/\langle C_f\rangle_\infty$ versus times for three values of D_f/D_p for which $\langle C_f\rangle_\infty$ is the asymptotic concentration obtained when the time goes to infinity. It is given by a simple mass balance between the PVC and the liquid and takes the following form

$$\langle C_f\rangle_\infty = \frac{\Delta r(2+\Delta r)}{K + \Delta r(2+\Delta r)}. \tag{43}$$

The average concentration rises up quickly at short times behaving as a square root of time. At large times, $\langle C_f\rangle(t)/\langle C_f\rangle_\infty$ goes to the unity. The numerical solutions obtained for increasing D_f/D_p are more and more close to the exact solution provided by Crank even if the numerical solution is achieved in cylindrical domain with small curvature.

This numerical example shows the accuracy of the numerical solution which can be

used to compare with solutions obtained in dynamic condition.

[1] J. Stoer and R. Bulirsch. *Introduction to numerical analysis*. Springer-Verlag, New York, 1993.

[2] E. Süli and D. F. Mayers. *An Introduction to Numerical Analysis*. Cambridge University Press, Cambridge (UK), 2003.

[3] W. Guo, G. Labrosse, and R. Narayanan. *The Application of the Chebyshev-Spectral Method in Transport Phenomena*, volume 68 of *Lecture Note in Applied and Computational Mechanics*. Springer-Verlag, Berlin, 2012.

[4] C. A. J. Fletcher. *Computational Techniques for Fluid Dynamics. Volume I: Fundamental and General Techniques*. Springer-Verlag, Berlin, 1991.

[5] H. S. Carslaw and J. C. Jaeger. Some two-dimensional problems in conduction of heat with circular symmetry. *Proc. Lond. Math. Soc. s2*, 46(1):361–388, 1940.

[6] H. S. Carslaw and J. C. Jaeger. *Conductions of heat in solids*. Clarendon Press, Oxford, second edition, 1959.

[7] G. De Vahl Davis. Natural convection of air in a square cavity: a bench mark numerical solution. *Int. J. Numer. Methods Fluids*, 3:249–264, 1983.

[8] J. Crank. *The mathematics of diffusion*. Clarendon Press, Oxford, 1956.